

# Superfluorescence from optically trapped calcium atoms

A. Kumarakrishnan\*

*Department of Physics, New York University, New York, New York 10003*

X. L. Han

*Department of Physics, Butler University, Indianapolis, Indiana 46208*

(Received 27 January 1998)

We have studied superfluorescence (SF) under highly unfavorable conditions of rapid collisional and radiative distribution in a Doppler-broadened medium. Nanosecond SF pulses at  $5.5 \mu\text{m}$  were generated on the Ca  $4s4p \ ^1P_1 - 3d4s \ ^1D_2$  transition from a column of calcium vapor buffered with Ar by optically pumping the  $4s^2 \ ^1S_0 - 4s4p \ ^1P_1$  transition. The Rabi frequency associated with the intense pump pulse prevents the occurrence of SF while the pump laser is on. As a result, the predicted scaling laws that describe the properties of SF in a transversely excited system, such as peak heights, pulse widths, and delay times, are shown to apply in our situation in which the conditions resemble swept excitation. The delay times were found to be in agreement with a fully quantum mechanical calculation which describes the initiation of SF. Measurements of the densities of the three levels, the absolute SF photon yield, and the spatial distribution of the excited states indicate that the system has a quantum yield of unity. The SF intensity increases with an increase in Ar pressure due to collisional redistribution until the collisional dephasing rate inhibits SF. The conditions describing the transition of SF to amplified spontaneous emission allow us to measure the collisional broadening rate for the SF transition. [S1050-2947(98)02611-0]

PACS number(s): 42.50.Fx, 42.50.Gy, 42.50.Md, 42.65.Tg

## I. INTRODUCTION

A collection of two-level atoms may be prepared in a coherent state by using an external source to establish the coherence. Alternatively, an initially inverted population may evolve from spontaneous emission into a coherent state by coupling through the common electromagnetic field of emitted radiation. The former is referred to as superradiance (SR), after Dicke who first calculated an enhanced radiative decay rate for microscopic arrangements of phased arrays of dipoles [1]. The latter process is now called superfluorescence (SF) [2]. Initially, SF begins as spontaneous emission with intensity proportional to the total number of excited radiators  $N$ , but as the dipoles couple, the intensity scales rapidly as  $N^2$ , analogous to SR. SF is distinguished by a finite delay time  $\tau_D \propto 1/N$  in which the coherence builds up.

In typical experiments, a population inversion is created in a three-level amplifier (Fig. 1). A pulsed laser (frequency  $\omega_L$ ) transfers population from level  $|0\rangle$  (ground state) to an excited state  $|1\rangle$ , which has a dipole-allowed transition to a lower level  $|2\rangle$ . The population in  $|1\rangle$  is contained in a cylindrical column or atomic beam. SF pulses that are highly directional evolve from quantum noise at the atomic frequency  $\omega_{12}$ . Since the peak intensity scales as  $N^2$ , the temporal width scales as  $1/N\Gamma_{12}$  where  $\Gamma_{12}$  is the spontaneous emission rate of uncoupled atoms.

SF has been extensively reviewed [3–6]. We will briefly describe aspects of SF that pertain to our results. Allen and Peters [7] differentiated Dicke superradiance from SF and

derived the threshold condition at which pure cooperative emission is expected to make a transition to a regime where the effects of propagation become important. This is the same as the Schawlow-Townes condition [8] for stimulated emission and holds for a mirror less single pass laser. The difference between a laser where the peak intensity is  $\propto N$  (stimulated emission) and SF where it is  $\propto N^2$  was described by Feld [9]. Stimulated emission will terminate when the population difference between  $|1\rangle$  and  $|2\rangle$  becomes zero, whereas all the atoms can be transferred to  $|2\rangle$  by SF. Other examples of  $N^2$  emission in large samples include optical free induction decay [10], and photon echoes [11], phenomena in which a very small fraction of the energy is radiated collectively [9]. These systems behave like an array of classical dipole oscillators that are driven in phase during the excitation, and therefore have an initial nonzero dipole moment (as in SR).

Calculations of SF pulse shapes distinguished a regime of ‘‘pure’’ SF [2], where, the evolution of the system is described by the sine-Gordon equation, which gives soliton solutions [(sech<sup>2</sup>) pulse shapes]. The statistical properties of such pulses showed that large scale fluctuations in SF intensity are a manifestation of quantum noise [12,13]. For this

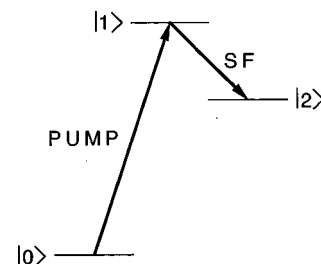


FIG. 1. Three-level system.

\*Present address: Research Laboratory of Electronics, MIT, Building 26, Room 268, 77 Massachusetts Ave., Cambridge, MA 02139.

reason, the stochastic properties of both SF, and stimulated Raman scattering (SRS), which occurs at the frequency  $\omega_L - \omega_{02}$ , have been studied for their potential as macroscopic amplifiers of quantum fluctuations [14]. Analytical descriptions of the competition between SRS and SF are described in [15,16].

The properties of SF are usually quantified [17] in terms of the radiative coupling time  $\tau_R$ , the propagation time for light through the medium  $\tau_E = L/c$ , the time delay  $\tau_D$  for onset of cooperative emission, and the dephasing time  $T_2$  in which the coherence is destroyed. The earliest SF experiments were performed in HF gas [18]. SF was generated with  $\tau_E < \tau_R \ll \tau_D < T_2$  which satisfied the conditions for ‘pure’ SF. In both the HF experiment [18] and later experiment in Cs [19], the dominant dipole dephasing mechanism was the Doppler effect. SF was also observed in Na [20], and TI [21] when  $T_2$  (due to Doppler dephasing) was less than  $\tau_D$ . SF experiments in CH<sub>3</sub>F [22] provide an alternate test where Doppler dephasing was negligible but the collisional dephasing time was smaller than  $\tau_D$ . Studies in collisionally perturbed Ba ( $6^1S_0 - 6^1P_1 - 5^1D_2$ ) [23] showed that strong SF emission can occur even when the natural radiative lifetime  $T_1$  ( $\sim 6$  ns) of the  $^1P_1$  states leads to  $T_2 < T_1 < \tau_D$ . This was due to rapid collisional redistribution ( $\sim 1$  ns), which increased the population transfer to the  $^1P_1$  level.

We report experimental studies of SF in a Ca ( $4^1S_0 - 4^1P_1 - 3^1D_2$ ), which extends these findings to even more extreme conditions. We show that SF can occur with a quantum gain of order unity even when  $T_2 < \tau_D$  and the branching ratio  $A_{P-S}/A_{P-D}$  of the pump and SF transitions is extreme ( $\sim 10^5$ ) [24]. An interesting aspect of the large oscillator strength for the pump transition is that the Rabi frequency  $\Omega$  for pumping seems to preclude the occurrence of SF while the pump laser is on. Although our system is pumped longitudinally, it behaves like a transversely pumped configuration.

Our results are best described in terms of the ratio  $L/L_c$  following [6]. Here,  $L$  is the sample length and  $L_c$  is the cooperation length that satisfies the Arecchi-Courten’s [25] criteria for pure SF.  $L_c$  is the maximum length over which a collection of uncorrelated excited atoms can attain a macroscopic polarization via spontaneous emission. To date, most SF experiments have studied the temporal ringing in SF pulse shapes, peak heights, and delay times in the regime of ‘pure’ SF with  $L/L_c < 1$ . Our experiment reports studies of these properties as well as quantum yields in the regime  $L/L_c > 1$ . Under these conditions, we show that the peak heights scale as  $N$  and the delay times scale as  $(1/N^{1/2})$ . In particular, we show that the delay times agree with predictions of a fully quantum-mechanical model that describes the initiation of SF.

The Ca experiment involves an optically trapped medium that increases the efficiency of SF. This is also the case in incoherently excited (by electron impact) copper vapor, which produces cooperative emission ( $\propto N^2$ ) [26]. SF-like phenomena have recently been observed in laser ionized media pumped by electron impact [27,28], in a magnetically confined recombining plasma column [29], and in Auger-pumped short-wavelength lasers [30]. References [26,30] are also examples of samples in which optical trapping results in cooperative emission on a less favorable radiative transition.

Related cooperative effects involving relativistic electrons have also been found to occur [31] in a free-electron laser.

The body of this paper is divided into three sections. Section II introduces background concepts. Section III describes experimental details and Sec. IV is a discussion of results.

## II. CRITERIA FOR SF

The radiative coupling time  $\tau_R$  [11] is the characteristic time in which the quantum-mechanical initiation of SF results in a classical field. It is the enhanced rate of emission due to a cooperative effects and is given by

$$\tau_R = \frac{1}{N\Gamma_{12}\mu}. \quad (1)$$

Here,  $N$  is the total number of participating atoms,  $\Gamma_{12}$  is the spontaneous emission rate for the SF transition, and  $\mu$  is a geometrical factor that defines the diffraction solid angle of the interacting volume. The effect of  $\mu$  (typically  $10^{-6}$  in the mid-IR region) is to reduce the rate of cooperative emission except along certain preferred spatial modes. For a thin cylindrical disk  $\mu = (3/8\pi)\lambda^2/A$ ; here,  $\lambda$  is the SF wavelength and  $A$  is the area of cross section of the excited states. The expression for  $\mu$  has to be modified for a long cylindrical column (radius  $r$ ) or for a thin slab with  $L \gg r \gg \lambda$ . However, the correction is small (of order unity) and is not required for a discussion of our results. Thus, the usual form of Eq. (1) is

$$\tau_R = \frac{8\pi AT_{12}}{3\lambda^2 N}, \quad (2)$$

where  $T_{12} = 1/\Gamma_{12}$  is the radiative lifetime of the SF transition. The delay time  $\tau_D$  for the onset of SF is functionally related to  $\tau_R$ ; its exact expression depends on the geometry and the dephasing.

The threshold for SF occurs when  $\tau_R$  is equal to the dipole dephasing time  $T_2$  [32]. Thus,  $\tau_R = T_2$  gives  $T_{12}/N\mu = T_2$ . Replacing  $N$  by the threshold number of atoms  $N_T$  and writing the volume of the sample as  $V_C = AL$ , we find

$$N_T = \frac{8\pi T_{12} V_C}{3T_2 \lambda^2 L}. \quad (3)$$

For swept excitation in a Doppler-broadened column, no upper limit on the number of atoms that can couple radiatively is expected [33] since SF initiated in time  $\tau_R$  follows the pump pulse at nearly the same speed. However, for transverse excitation in an atomic beam, pure SF can take place in a column of length  $L$  only if  $\tau_E < \tau_R$  [25]. This would enable atoms at one end of the sample to communicate with atoms at the other end during the evolution of the system. Thus it is required that  $L/c < 1/N\Gamma_{12}\mu$ . This yields an upper limit for the maximum cooperation number  $N_c$ , which is the largest number of atoms that can emit cooperatively. Thus,

$$N_c < \frac{8\pi A c T_{12}}{3\lambda^2 L}. \quad (4)$$

Equation (4) derived in [25] is equivalent to the threshold condition derived by Schawlow and Townes [8]. A number

of regimes for SF can be argued around this limit for the case of transverse pumping [2,6]. As previously noted, our system behaves as if transversely pumped because SF is rapidly dephased by the Rabi frequency of the pump pulse.

So long as  $\tau_E < \tau_R$  we can have pure SF. The SF peak intensity is  $\propto N^2$  and the pulse width scales as  $1/N\Gamma_{12}$ . In this case, it has been shown that the delay time  $\tau_D \propto 1/N$  [34]. When  $\tau_E > \tau_R$ , i.e.,  $N > N_c$ , the effects of propagation become important and the SF peak intensity becomes  $\propto N$ . These are the conditions addressed in our work.

In the latter case, we follow [6], and consider the column of length  $L$  to be divided into  $S$  noninteracting slices, each of which emits cooperatively. The emission from the sample can be treated as an incoherent sum of these emissions. Each slice of length  $L_c$  contains  $N'$  atoms such that

$$S = \frac{L}{L_c} = \frac{N}{N'} = \frac{\tau_{R'}}{\tau_R}. \quad (5)$$

Here, the SF evolution time  $\tau_{R'}$  in each slice just satisfies the condition derived in [25], i.e.,  $L_c/c = \tau_{R'}$ .  $L_c$  is the maximum value of the Arecchi-Courtens length [25]. The number of slices can now be expressed as

$$S = \left( \frac{\tau_E}{\tau_R} \right)^{1/2}. \quad (6)$$

From Eqs. (5) and (6), it can be seen that  $\tau_{R'}$  is the geometrical mean of  $\tau_E$  and  $\tau_R$ , i.e.,  $\tau_{R'} = (\tau_R \tau_E)^{1/2}$ . For  $L > L_c$ , the SF pulse width from the entire sample was shown to scale as  $(1/N^{1/2}\Gamma_{12})$  and the delay time, being proportional to  $\tau_{R'}$ , scales as  $(1/N^{1/2})$  [6].

It is now possible to describe SF in terms of  $L_c$ ,  $L$ , and the SF threshold length  $L_T$  (which corresponds to  $N_T$ ) [2].  $1/L_T = \alpha_0$  is the gain coefficient at frequency  $\omega_{12}$ . Let us first consider the case  $L_T \ll L < L_c$ .  $L_T \ll L$  implies that the dipole dephasing time  $T_2$  is larger than the system evolution time  $\tau_R$ , i.e.,  $\tau_R \ll T_2$ . This means that the small signal gain along the excited column [35] given by

$$\alpha_0 L = \frac{2T_2}{\tau_R} \quad (7)$$

is much larger than unity. For pure SF, there is virtually no dephasing during the delay time in which the system evolves (typically,  $\tau_D \sim 100\tau_R$ ). If  $T_2 < \tau_D$  SF can still occur as long as the gain is sufficiently large and this is referred to as damped SF. The delay times and pulse widths are expected to be larger than in the absence of dephasing. It has been shown [36] that the emission is SF if

$$T_2 > (\tau_R T_D)^{1/2}, \quad (8)$$

where  $T_D$  is the delay time  $\tau_D$  in the absence of dephasing. When

$$\tau_R < T_2 < (\tau_R T_D)^{1/2}, \quad (9)$$

the emission reverts to incoherent spontaneous emission in which case the dipoles are dephased before cooperative emission can take place. The excited column behaves like a collection of independent dipoles. The emission also loses

the highly directional character of SF and the signal intensity detected along the column axis can decrease by several orders of magnitude. It is, however, possible that the spontaneous emission can be amplified along the length of the column, in which case it can be directional. This is known as amplified spontaneous emission (ASE). In this case, the pulse is expected to have no time delay and consist of a series of random spikes, which on averaging, gives the exponential decay of the upper level population. The transition from SF to ASE has been discussed in [36–38] and has been observed in [39].  $L < L_c$  implies that cooperative emission dominates effects of propagation. The peak intensity is  $\propto N^2$ .

When the conditions  $L_T \ll L_c < L$  are fulfilled, the effects of propagation can be expected to dominate. It must be noted, however, that SF from a collection of uncorrelated slices is fundamentally different from pure stimulated emission. Whereas in the former situation, all  $N$  atoms in level  $|1\rangle$  can be transferred to level  $|2\rangle$ , in the latter, the emission ends when the populations of the two levels are equalized. Our measurements at high density in this regime show that SF has a quantum gain of unity rather than 0.5. It has been argued [40] that SF must satisfy the condition  $\alpha_0 L_c \gg 1$  in all regimes, whereas stimulated emission occurs when  $\alpha_0 L \gg 1$ ,  $\alpha_0 L_c \ll 1$ .

It has so far been assumed that the initiation of SF begins after an incoherent excitation of level  $|1\rangle$ , i.e., there is no initial dipole moment at the SF frequency  $\omega_{12}$ . This corresponds to a very restrictive condition that the pump pulse should have an area  $\pi$  and an infinitesimally small duration  $\tau_P$  such that  $\tau_P < \tau_R$  [41]. A pump pulse with Rabi frequency  $\Omega$  such that

$$\tau_P > \tau_R, \quad \Omega \tau_R > 1, \quad \Omega T_1, \quad \Omega T_2 > 1 \quad (10)$$

can produce an initial coherence at the SRS frequency  $\omega_L - \omega_{02}$  that can significantly alter the evolution of the population of level  $|1\rangle$ . The situation is then analogous to SR rather than to SF. The peak intensity of the pulse is  $\propto N^2$  and its delay time  $\tau_D$  is expected to be shortened.  $\tau_D$  becomes a function of both  $\tau_R$  and  $\tau_P$  in this case [41], and the pulse shapes and statistics of the fluctuations are considerably modified. Emission in the ‘‘forward direction’’ was expected to dominate.

### The calcium experiment

The experiment was done in a 50-cm column of Ca vapor buffered with argon. When the  $4s^2 \ ^1S_0 - 4s4p \ ^1P_1$  transition is pumped near resonance with a pulse 12 ns in duration, collisionally aided SF is observed at 5.5  $\mu\text{m}$  on the  $4s4p \ ^1P_1 - 3d4s \ ^1D_2$  transition (Fig. 2). The estimated values for  $N_T$  [Eq. (3)] and  $N_c$  [Eq. (4)] are  $3 \times 10^{10}$  and  $1.3 \times 10^{11}$ , respectively. The scaling laws for peak intensities and delay times were studied by varying the SF photon number ( $N$ ) between  $2 \times 10^{11}$  and  $1 \times 10^{14}$  at an Ar pressure of 1 Torr.  $N$  was varied by changing the pump laser detuning or by varying the ground-state density. The corresponding variation in the number of slices  $S$  was between 1.5 and 30. The peak intensity was observed to scale as  $N^2$  when  $S$  is small. As  $S$  increases, the peak intensity scales as  $N$  and the delay times and pulse widths show a  $1/\sqrt{N}$  dependence.

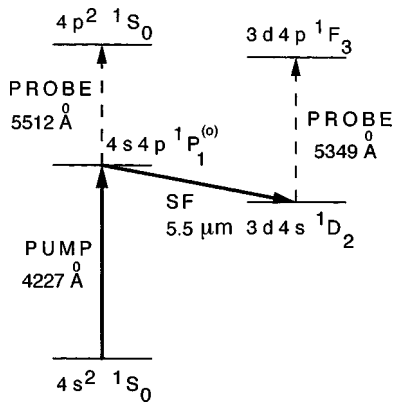


FIG. 2. Ca three-level system showing energy levels for pump-probe experiment to measure number densities.

The duration of the pump pulse (12 ns) is of the same order as the natural lifetime of the  $^1P_1$  level ( $T_1=4.6$  ns [42]), and the dephasing time  $T_2$  (for the SF transition). The branching ratio for the decay from  $^1P_1-^1S_0$  is  $\sim 10^5$  times larger [24] than that of the decay from  $^1P_1-^1D_2$  (the radiative rate for the SF transition  $\Gamma_{12}$  has been measured [43] to be  $3.68 \times 10^3 \text{ s}^{-1}$ ; the lifetime of the metastable  $^1D_2$  state is  $\sim 1$  ms [44]). Although SF evolves under conditions when  $T_2 < \tau_D$ , it was found to have a quantum gain of unity at high density. This is consistent with estimates for  $\alpha_0 L_c$  using Eq. (7) ( $\alpha_0 L_c$  varies between 10 and 250).

Also significant is the observed range in  $\tau_D$ , which varies from  $\sim 12$  ns for large  $N$  to  $\sim 50$  ns for small  $N$ , i.e.,  $\tau_D \gg T_1$ . SF can occur with high efficiency over this time scale because radiation trapping preserves the column of excited states. The mean free path of photons  $\ell$ , at the pump wavelength, estimated as the inverse of the absorption coefficient  $K_0$  at line center, varies between  $\sim 350 \mu\text{m}$  (at low density) and  $\sim 15 \mu\text{m}$  (at high density). Consequently, the initial area of cross section of excited states ( $2.8 \times 10^{-2} \text{ cm}^2$ ) defined by the pump laser can be expected to increase by about 3% in 12 ns and by  $\sim 50\%$  in 50 ns. This is consistent with predictions for an infinite slab of optically trapped atoms [45]. The saturation of  $\tau_D$  at  $\sim 12$  ns is attributed to the Rabi rate  $\Omega$  ( $\sim 3 \times 10^{11} \text{ Hz}$ ) at the pump frequency ( $1/\Omega < \tau_R, \tau_R'$ ). This factor as well as the small radiative rate for the SF transition probably prevent the occurrence of SF for the duration of the pump pulse. Hence the scaling laws correspond to a transversely excited sample.

The intensity of SF was observed to increase substantially with an increase in Ar pressure until the value of  $T_2$  is small enough to preclude cooperative emission. The properties of the transition from SF to ASE described by Eqs. (8) and (9) allow us to infer the collisional broadening rate for the SF transition.

### III. EXPERIMENTAL DETAILS

The calcium vapor column was effectively constrained between knife edge baffles in a heated stainless steel cell pumped by a diffusion pump. The cell was pumped to  $8 \times 10^{-8}$  Torr and sealed with a small amount of buffer gas, usually 1 Torr of Ar (research purity  $>99.9995\%$ ). The Ar was necessary for preventing the cell windows from being coated with Ca. The Ar pressure was measured by a capaci-

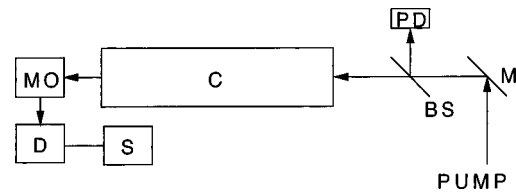


FIG. 3. Schematic of experiment. C, cell with Ca and Ar; BS, beam splitter; PD, photodiode; M, mirror; MO, spectrometer or bandpass filter; D, detector; S, oscilloscope.

tance manometer calibrated to  $\pm 0.2\%$ . The temperature of the cell was held uniform ( $\pm 2 \text{ }^\circ\text{C}$ ). Figure 3 shows the experimental setup.

The Ca column was longitudinally pumped by pulses from a multimode (1–2-GHz bandwidth) homemade dye laser tuned to the  $4s^2 \ ^1S_0-4s4p \ ^1P_1$  principal resonance line at  $4227 \text{ \AA}$ . The dye laser was pumped by a frequency tripled (355 nm) commercial YAG laser with a repetition rate of 10 Hz. The excitation pulses ( $>99\%$  linear polarization) had a Gaussian spatial profile, a full width at half maximum (FWHM) of 6 ns, and an average pulse energy of 1.5 mJ as measured with a Thermopile ( $\pm 2\%$ ). The pump was apertured to produce a top hat profile in the cell and collimated to have a confocal parameter greater than the length of the cell.

The SF pulses were incident on a Ge:Hg detector, which had a home-built transmission line. The crystal was cooled to  $\sim 30 \text{ K}$  by a cryorefrigerator. The bandwidth of the detector was assessed to be  $\geq 350 \text{ MHz}$ , which is probably an underestimate of its true performance in the mid IR. The detector output was connected to a 1 G sample/s digitizing oscilloscope. The pump pulse was detected by a 1.8-GHz commercial photodiode or a homemade photodiode assembly ( $\sim 500 \text{ MHz}$  bandwidth). The peak height and area under the pump pulse were held constant to within  $\pm 10\%$  during the experiment. Several different IR emissions were induced under different experimental conditions. These emissions were spectrally resolved with suitable IR bandpass filters and/or a  $\frac{3}{4}$ -m spectrometer with a 75-groove/mm grating blazed for  $10 \mu\text{m}$ .

The absolute yield of SF photons was measured with a LiTaO<sub>3</sub> pyroelectric detector calibrated ( $\pm 15\%$ ) against the Thermopile. This detector and its home-built pulse shaping amplifier had  $\sim 1$ -nJ energy resolution at a signal-to-noise ratio=1. This was sufficient to study the  $5.5\text{-}\mu\text{m}$  SF, which produced combined forward and backward emissions of pulse energies  $\sim 3.5 \mu\text{J}$  when  $[\text{Ca}(4 \ ^1P_1)] \sim 10^{14} \text{ cm}^{-3}$ . The ground-state density was determined by measuring the integrated linewidth [46] of the pump transition. This involved scanning the pump laser across the absorption profile and measuring the transmitted intensity.

The photon yields and temporal pulse shapes were recorded for various pump laser detunings at several values of the ground-state density. This made it possible to measure the time delays as a function of  $N$ . These measurements were done at the back end of the cell. It was difficult to determine the SF intensity at the front end of the cell since a suitable dichroic mirror was not available. Efforts to use a Ge filter as a mirror were only partially successful since the intensity of the pump laser was sufficient to damage the filter. In some of our studies, we used CaF<sub>2</sub> beam splitters to deflect the SF onto the detector at both ends of the cell. A comparison of

TABLE I. Representative measurements for 5.5- $\mu\text{m}$  SF with 1 Torr Ar [ $^1S_0$ ]-ground-state density;  $N$ , SF photon yield;  $\tau_R$ , dipole coupling time for entire column;  $S$ , number of slices;  $N'$ , number of SF atoms in slice;  $\tau_{R'}$ , dipole coupling time for slice;  $\Delta$ , pump laser detuning.

	$[^1S_0]$ ( $\text{cm}^{-3}$ )	$N$	$\tau_R$ (s)	$S$	$N'$	$\tau_{R'}$ (s)	$\Delta$ ( $\text{cm}^{-1}$ )
1	$8.8 \times 10^{12}$	$2.9 \times 10^{11}$	$7.2 \times 10^{-10}$	1.5	$1.9 \times 10^{11}$	$1.1 \times 10^{-9}$	-1
2	$8.8 \times 10^{12}$	$5.8 \times 10^{11}$	$3.6 \times 10^{-10}$	2.2	$2.6 \times 10^{11}$	$7.8 \times 10^{-10}$	0
3	$7.4 \times 10^{13}$	$1.3 \times 10^{13}$	$1.6 \times 10^{-10}$	10	$1.3 \times 10^{12}$	$1.6 \times 10^{-10}$	0
4	$2.3 \times 10^{14}$	$5.2 \times 10^{13}$	$4 \times 10^{-12}$	20	$2.6 \times 10^{12}$	$8.2 \times 10^{-11}$	0

pulses from both ends obtained on a single shot showed that the time delays were nearly identical. In addition, the time delays were the same for time-averaged pulses. The average photon yields measured at both ends after the SF was reflected by the Ge beam splitter were found to be identical within  $\pm 25\%$ . We therefore assume that the photon yields from both ends of the cell are the same.

Absolute measurements of the excited-state densities [ $\text{Ca}(4^1P_1)$ ] and [ $\text{Ca}(3^1D_2)$ ] were made to compare the photon yield with the number of excited atoms. The densities were measured by the equivalent width technique using a second, tunable, pulsed (probe) laser. This laser produced 5 ns (FWHM) pulses. The probe laser was scanned over the  $4s4p^1P_1-4p^2^1S_0$  line at 5512  $\text{\AA}$  and the  $3d4s^1D_2-3d4p^1F_3$  line at 5349  $\text{\AA}$  (Fig. 2), respectively. By delaying the probe suitably with respect to the pump, the densities of the excited states could be monitored before and after the evolution of the SF pulse. A detailed discussion of these measurements and experimental uncertainties is presented in [47].

The density of excited states was also measured by spatially translating the probe beam with respect to the pump beam. Thus, we were able to confirm that the size of the distribution of excited states was consistent with estimates based on the initial cross section defined by the pump laser's spatial profile. The SF divergence also gave an independent estimate of the size of the excited column. This estimate was important at low densities ( $10^{10}-10^{12} \text{ cm}^{-3}$ ) for which the equivalent width method was error prone.

## IV. RESULTS AND DISCUSSION

### A. Experimentally observed regimes

The number of independent slices  $L/L_c$  in the column was varied between  $\sim 1.5$  and 30 by varying  $N$ . Table I shows the ground-state density, the measured photon yield  $N$ , the coupling time  $\tau_R$  for the column, the number of slices  $S$ , the number of participating atoms in each slice  $N'$ , and the coupling time for the slice  $\tau_{R'}$  for a few measurements. As expected, the SF peak height scaled quadratically when  $S$  is small (rows 1 and 2) and linearly when  $S$  is larger (rows 3 and 4).

Figure 4 shows the average SF peak intensity as a function of pump detuning. The ground-state density was  $\sim 3 \times 10^{14} \text{ cm}^{-3}$ . In this case, the SF was imaged onto a Ge:Au detector after passing through a filter. With a 50% neutral density filter placed in the pump beam, the SF peak intensity decreases linearly at small detunings (large  $S$ ) and

quadratically at large detunings (small  $S$ ). This provides evidence for the change in scaling of the peak heights as a function of  $N$ .

### B. Quantum yield

The ground-state density measured as a function of the cell temperature [47] was verified to agree within error bars with values from vapor pressure curves [48]. Table II summarizes measurements for the size of the column of excited states (along one dimension) at three cell temperatures. The collimated pump beam had a top hat profile that was determined by scanning a pinhole across the beam. This measurement was corroborated by spatial profiles of the excited states measured by the probe laser at high cell temperatures and is shown in rows 2 and 3. The profile of  $^1P_1$  states was measured by probing just before the SF pulse. The  $^1D_2$  profile was probed within 10 ns after the peak of the SF pulse. Due to radiation trapping, the volume of the excited  $^1P_1$  column was estimated to change by less than 5% in the time the SF evolved. The spatial profiles of the excited states are consistent with these estimates. At lower temperatures, the density of excited states measured using the method of equivalent widths was error prone. In this case, the cross section of the excited column was inferred from measurements of the SF divergence. Its value in row 1 reflects the

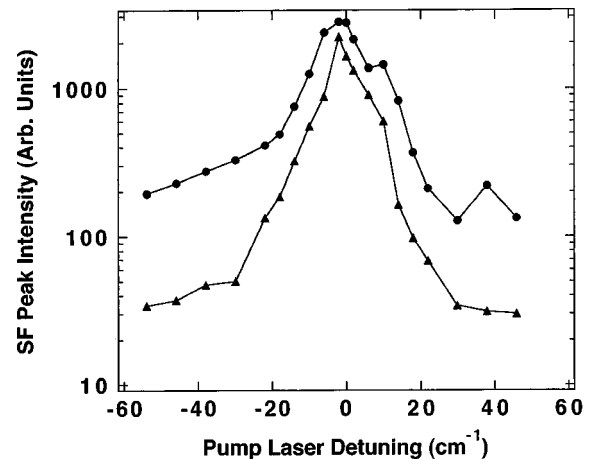


FIG. 4. Average SF peak intensity (512 pulses) as a function of pump laser detuning with 1 Torr Ar. [ $^1S_0$ ] $\sim 3 \times 10^{14} \text{ cm}^{-3}$ ; dots, with unattenuated pump; triangles, with 50% neutral density filter in pump; points have been connected to aid the eye; SF peak intensity scales quadratically at large detunings and linearly at small detunings.

TABLE II. Summary of measurements of the size of the excited column along one transverse dimension. Profiles of  $^1P_1$  and  $^1D_2$  states were measured by probing before and after the SF pulse, respectively; area of cross section of the pump beam gives the initial size of the excited column.

	Cell temperature ( $\pm 2$ K)	Pump beam (cm) ( $\pm 10\%$ )	$^1P_1$ Spatial profile (cm) ( $\pm 50\%$ )	$^1D_2$ Spatial profile (cm) ( $\pm 50\%$ )	From SF divergence (cm) ( $\pm 10\%$ )
1	798	0.19			0.36
2	848	0.19	0.2	0.2	0.14
3	923	0.19	0.25	0.15	0.07

expansion of the column in  $\sim 50$  ns in which the SF evolves, and is once again consistent with estimates.

Table III shows the  $5.5\text{-}\mu\text{m}$  SF photon yield, the densities of the ground and excited states, and the number of  $^1P_1$  atoms in the column just before SF emission for the same cell temperatures as in Table II. The pump laser was tuned on resonance for these measurements. The data have been corrected for systematic errors and the random errors are given separately for each measurement. In all cases, the probe laser delay was adjusted to measure the  $^1P_1$  density just before the evolution of SF. The initial volume of the column of excited states was estimated as  $1.4\text{ cm}^3$  for a length  $L = 50$  cm using measurements of the area of cross section ( $2.8 \times 10^{-2}\text{ cm}^2$ ) of the pump beam. This was used to estimate the number of  $^1P_1$  atoms in the column just before SF emission (for data in rows 2 and 3). For row 1, the SF divergence was used to estimate this number.

Our measurements show that the system has a quantum yield of unity at high density. In the presence of the large Rabi frequency of the pump, the system supports multiphoton processes which transfer population between levels  $|0\rangle$  and  $|1\rangle$ . In addition, collisionally aided absorption populates the  $m_j$  levels of the  $^1P_1$  state during the pump pulse. After the pump turns off, typically  $\frac{1}{5}$  of the population of the ground state was measured in the  $^1P_1$  level. Nearly all the atoms in the  $^1P_1$  state are then transferred by SF emission to the  $^1D_2$  level. At low density, the quantum yield is reduced to about 0.2 presumably on account of dephasing. This experiment reports systematic measurements of SF quantum yield.

TABLE III. Measurements of the SF quantum yield. The  $^1P_1$  density was measured just before the evolution of SF. The number of  $^1P_1$  atoms was estimated from measurements of the volume of excited atoms. The quantum yield is of order unity for entries 2 and 3.

	Cell temperature ( $\pm 2$ K)	$[^1S_0]$ ( $\text{cm}^{-3}$ ) ( $\pm 30\%$ )	$[^1P_1]$ ( $\text{cm}^{-3}$ )	Photon yield $N_{\text{SF}}$ ( $\pm 15\%$ )	$^1P_1$ atoms in column	SF Delay time (ns) ( $\pm 0.7\%$ )
1	798	$1.1 \times 10^{13}$	$5.2 \times 10^{11}$ ( $\pm 75\%$ )	$5.8 \times 10^{11}$	$2.8 \times 10^{12}$ ( $\pm 95\%$ )	46
2	848	$9.6 \times 10^{13}$	$1.1 \times 10^{13}$ ( $\pm 35\%$ )	$1.3 \times 10^{13}$	$1.5 \times 10^{13}$ ( $\pm 55\%$ )	15
3	923	$3.0 \times 10^{14}$	$3.8 \times 10^{13}$ ( $\pm 35\%$ )	$5.2 \times 10^{13}$	$5.3 \times 10^{13}$ ( $\pm 55\%$ )	12

### C. Time delays

Figure 5 shows a representative single shot trace of the pump pulse and the SF pulse. The observed time delays  $\tau_D$  (with 1 Torr Ar) are shown in Fig. 6(a) as a function of the total number of SF photons  $N$ . Values for the time delay represent the time between the onset of triggering the oscilloscope at the leading edge of the pump pulse (10% point) and the peak of the SF pulse averaged over 512 repetitions. The errors in these measurements are assessed as  $\pm 0.7$  ns— one-half the quadrature sum of the digitization period and the rise time of a 500-MHz bandwidth-limited signal. The values of  $N$  have uncertainties of  $\pm 15\%$ .

Polder *et al.* [49] have calculated the SF delay time in the absence of dephasing as

$$T_D \approx \tau_R \left[ \frac{1}{4} \ln 2 \pi N \right]^2 \quad (11)$$

for the regime  $L/L_c < 1$  using a fully quantum-mechanical model. The model assumes a delta-function excitation at  $t = 0$  and a constant number of participating atoms  $N$ . For  $L/L_c > 1$ , we have replaced  $\tau_R$  by the slice evolution time  $\tau_{R'}$  and  $N$  by the number of atoms in each slice,  $N'$ . The time delays for each slice calculated from

$$T_D = \tau_{R'} \left[ \frac{1}{4} \ln 2 \pi N' \right]^2 \quad (12)$$

are shown in Fig. 6(a) as the solid curve. For small  $N$ , the experimental time delays  $\tau_D$  show the expected  $1/\sqrt{N}$  dependence predicted by Eq. (12) and lie consistently above this

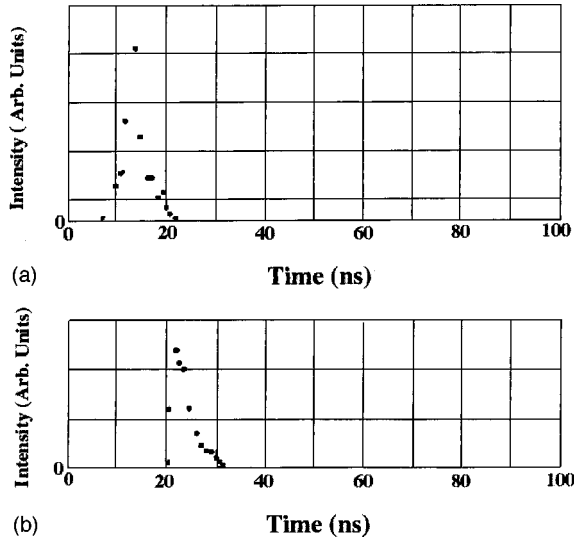


FIG. 5. Single shot oscilloscope record; number of slices  $N = 10$ ; (a) pump pulse, (b) corresponding SF pulse.

value. The dashed line represents the  $1/N$  dependence predicted by Eq. (11). The same data are displayed on a log-log plot in Fig. 6(b).

The experimental delay times in Fig. 6 are a result of the time ( $\sim \tau_{R'}$ ) in which the dipole moment builds up in each uncorrelated slice. The long delays are due to the small radiative rate ( $\Gamma_{12} \approx 3.68 \times 10^3 \text{ s}^{-1}$ ) of the ( $^1P_1 - ^1D_2$ ) SF transition. At early SF initiation times, the effects of both homogeneous and inhomogeneous dephasing can be expected to result in  $\tau_D > T_D$ . However, the Doppler dephasing rate of the SF transition is much larger than the collisional dephasing rate at an Ar pressure of 1 Torr (as shown later).

The Doppler width of the SF transition ( $\gamma_D \sim 186 \text{ MHz}$  at a temperature  $T = 925 \text{ K}$ ) and the radiative dephasing rate of  $|1\rangle$  ( $\Gamma_1/2 \sim 1.1 \times 10^8 \text{ s}^{-1}$ ) suggest a dephasing time  $T_2 \sim 3.3 \text{ ns}$ . In Appendix A of [47], we discuss the role of radiation trapping on the evolution of SF based on numerical simulations [50]. At low density, only atoms in a particular velocity group corresponding to the natural linewidth of the SF transition  $\Gamma_{\text{SF}} = \Gamma_1/2\pi \sim 35 \text{ MHz}$ , are expected to take part directly in SF. This is a fraction  $F = \Gamma_{\text{SF}}/\gamma_D \sim 1/5.3$  of the atoms under the Doppler profile. Atoms in other velocity groups are reshuffled in and out of this dominant group due to radiation trapping at the pump frequency and therefore participate indirectly. Thus the actual dephasing rate for SF should probably be given by  $\Gamma_2 = \Gamma_1/2 + \gamma_D/5.3 \sim 1.4 \times 10^8 \text{ s}^{-1}$ . This corresponds to a dephasing time  $T_2 \sim 7 \text{ ns}$ . Our experiments thus fall in the regime of damped SF where  $\tau_{R'} < T_2 < \tau_D$ .

Schuermans *et al.* [4] accounted for the effect of Doppler dephasing on the delay times  $T_D$  in Eq. (12). Their expression for the experimental delay time is

$$\tau_D = T_D \left[ 1 + \frac{\sqrt{\tau_{R'} T_D}}{T_{2 \text{ Doppler}}} \right]. \quad (13)$$

The value of  $\tau_D$  from Eq. (13) with  $T_{2 \text{ Doppler}} = 29 \text{ ns}$  [or  $1/(35 \text{ MHz})$ ] is shown as the dotted line in Fig. 6. While the agreement with experiment appears satisfactory, it would

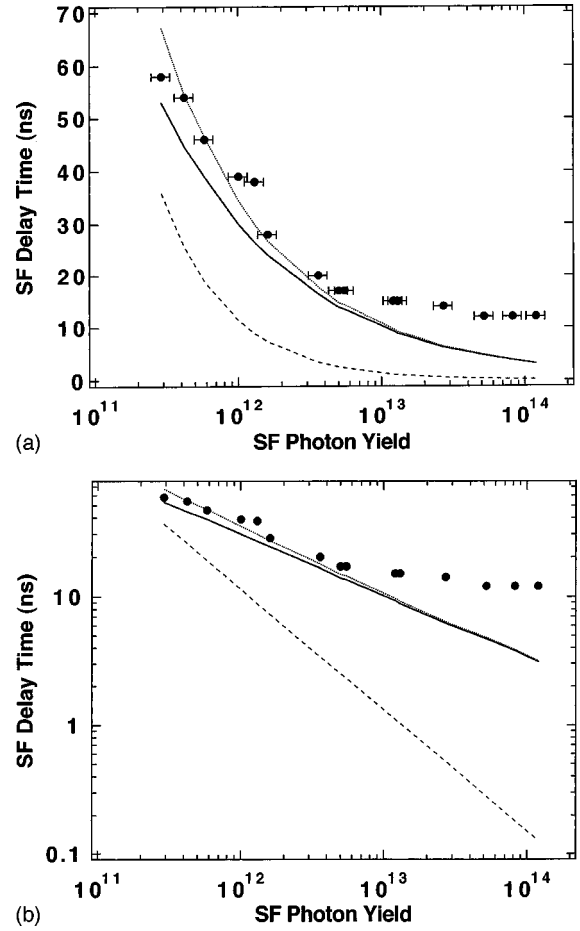


FIG. 6. (a) SF delay time as a function of the measured SF photon yield  $N_{\text{SF}}$  (error bars of  $\pm 15\%$ ). Solid curve,  $1/\sqrt{N}$  dependence predicted by Eq. (12). Dotted curve, includes effect of Doppler dephasing given by Eq. (13). Dashed curve,  $1/N$  dependence predicted by Eq. (11). (b) Same data on a log-log plot. The duration of the pump pulse is 12 ns.

still be necessary to quantify additional effects due to the coherence induced by the pump pulse on shortening the delay times.

In this context, we note that the predictions of [51] based on a mean field theory significantly underestimate the delay time. Therefore, the modification of this theory in [41] to account for the coherent effects of the pump pulse (which are expected to shorten the SF delay) does not provide a valid quantitative estimate. We have also inferred that such effects are small since no tunable emission at the SRS frequency  $\omega_L - \omega_{02}$  or significant asymmetry between forward and backward emissions were observed. SF time delays were observed to level off at 12 ns, which is nearly the total duration of the pump pulse. This is consistent with the expectation that the Rabi frequency of the pump laser will modify the evolution of SF.

#### D. Transition to ASE

Figure 7 shows a log-log plots of  $\sqrt{\tau_{R'} \tau_D}$  (data) and  $\sqrt{\tau_{R'} T_D}$  (solid line) as a function of  $N$ , at an Ar pressure of 1 Torr. The horizontal dashed line is the previously estimated value ( $T_2 = 7 \text{ ns}$ ) at which the SF-ASE transition was ex-

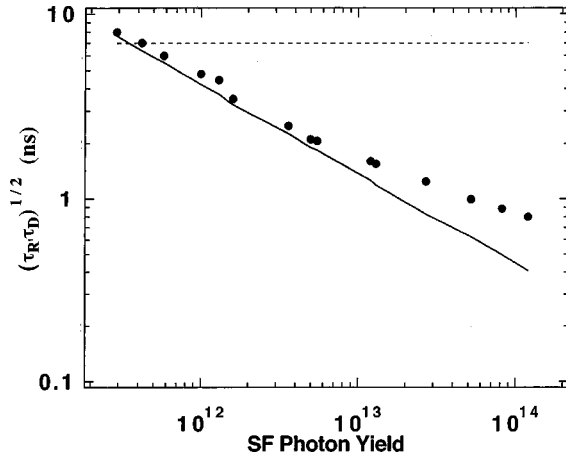


FIG. 7. Log-log plot of  $\sqrt{\tau_{R'} \tau_D}$  as a function of the measured SF photon yield.  $\tau_D$  is the average experimental delay time shown in Fig. 6. The solid line represents  $\sqrt{\tau_{R'} \tau_D}$  with  $T_D$ , given by Eq. (12). The horizontal dashed line represents  $T_2 = 7$  ns.

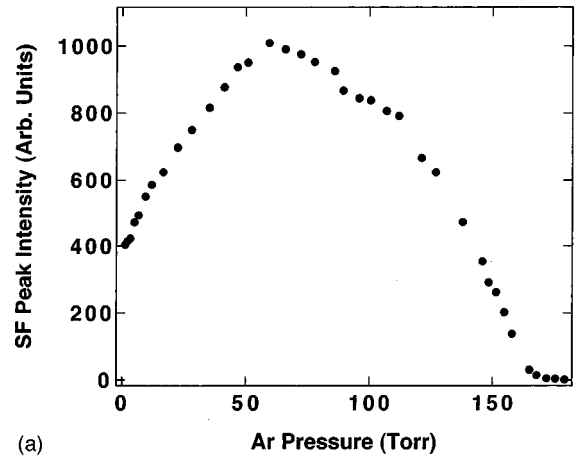
pected to occur. The data suggest that  $T_2$  is larger than the estimated value. This would only improve the agreement between the predictions of Eq. (13) and the experimentally observed delay times in Fig. 6.

We were able to test the effects of collisional dephasing by increasing the Ar pressure and observing the transition from SF to ASE. Figure 8(a) shows the time averaged SF peak intensity as a function of Ar pressure at a ground-state density of  $8 \times 10^{13} \text{ cm}^{-3}$ . Initially, the SF intensity increases due to increased collisional transfer of population to all magnetic sublevels of the  $^1P_1$  level from the dressed levels created by the pump laser. The ratio of populations in the  $m_J = 0$  and  $m_J = \pm 1$  levels are governed by collision cross sections for the transfer of populations from the dressed levels. These cross sections are parametrized by  $\Omega/\Delta$ , where  $\Omega$  and  $\Delta$  are the Rabi frequency and detuning of the pump laser, respectively. At higher pressures, collisional dephasing suppresses SF. The SF intensity also shows a nonzero intercept at zero Torr, suggesting that multiphoton processes play an important role in populating the  $^1P_1$  level. SF recorded without Ar also supports this conclusion. Figure 8(b) shows corresponding SF time delays as a function of Ar pressure. The initial decrease is due to the increase in  $N$  effected by collisional transfer. The time delays and pulse widths subsequently increase on account of collisional dephasing.

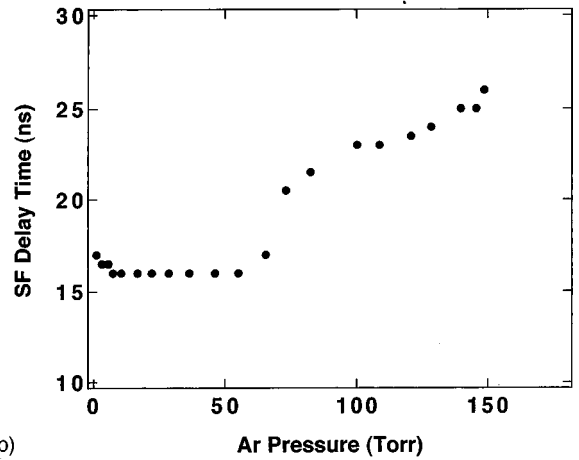
As discussed in Sec. II [Eq. (9)], it has been shown [36] that when  $\tau_{R'} < T_2 < \sqrt{\tau_{R'} \tau_D}$ , SF changes to ASE. We have used this to estimate the collisional dephasing rate  $\gamma_C = CP$  by measuring the Ar pressure  $P$  at which SF is dephased. Here,  $C$  is a constant. Assuming that

$$\frac{1}{T_{2\text{ASE}}} \sim \frac{1}{\sqrt{\tau_{R'} \tau_D}} = \frac{\gamma_D}{5.3} + \frac{1}{2T_1} + \gamma_C \quad (14)$$

we can find the value of  $C$  (in units of  $\text{s}^{-1}/\text{Torr}$ ) from the pressure  $P$  at the transition to ASE. We estimate  $\gamma_C \sim 7.9 \times 10^5 \text{ s}^{-1}$  at 1 Torr, using the photon yields for the data in Fig. 8(a) and the measured time delays in Fig. 8(b). Similar estimates for  $\gamma_C$  were also obtained at other ground-state densities. Thus, the inferred value of the collisional dephas-



(a)



(b)

FIG. 8. (a) SF peak intensity (average of 512 pulses) as a function of Ar pressure;  $[^1S_0] \sim 8 \times 10^{13} \text{ cm}^{-3}$ ; pump laser detuning  $\Delta = 0.5 \text{ cm}^{-1}$ . (b) Average SF delay time as a function of Ar pressure.

ing rate at 1 Torr is  $\sim 50$  times smaller than the Doppler dephasing rate as mentioned previously.

## E. Conclusions

Our results confirm scaling laws predicted in [6] for the regime  $L/L_c > 1$ . This experiment also confirms the predictions for SF time delays based on a fully quantum-mechanical model [49] in the above regime. Our measurements at high densities indicate that after the termination of the pump pulse, almost all the atoms in the  $^1P_1$  level are transferred to the  $^1D_2$  level. This constitutes a quantum gain of unity and demonstrates that SF is a robust process even in the presence of rapid dephasing effects [52]. The Ca SF amplifier could be potentially useful in achieving efficient sources of radiation in the mid-IR for use as a diagnostic tool to determine species concentration in diverse environments such as the upper atmosphere (Raman LIDAR systems) and plasma torches. The uncertainties in our density measurements may be improved by time-resolved studies of  $^1P_1$  and  $^1D_2$  populations with cw tunable diode lasers, which have now become available at suitable wavelengths. We have measured the SF dephasing time using the results of [36] and shown that the properties of the SF-ASE transition may be used to measure collisional broadening rates. Related experiments include studies of level degeneracy on SF polarization

[53], and temporal ringing in collisionally induced SF pulses at  $1.9 \mu\text{m}$  on the  $3d4S^3D_J-4s4p^3P_{J-1}$  transitions [54] (temporal ringing is an intrinsic property of SF even for  $L/L_c < 1$  as shown in [55]). A survey of SF cascades generated by populating near Rydberg levels is summarized in [56].

The effect of anomalous light scattering by quantum fluids in the vicinity of a phase transition is now a well-known effect. Since SF is very sensitive to dephasing parameters, it could be used to monitor abrupt changes in order parameters of these systems. This property of SF may become relevant following the recent demonstration of Bose-Einstein condensation [57] using laser cooling techniques. With the advent of efficient atomic traps [58], the possibility of demonstrat-

ing striking effects in small sample SF [6] may have become realistic. These include the effects of Van der Waals dephasing on the coherent evolution of small samples and the collective behavior of just two or three atoms.

#### ACKNOWLEDGMENTS

This work was supported by grants from the NSF PYI, NSF EPSCOR (Idaho), and AFWL. A.K. would like to thank John Carlsten of Montana State University for helpful discussions on the scaling laws of SF with reference to the results described in [38]. A.K. would also like to acknowledge discussions with Jim Kelly.

- 
- [1] R. B. Dicke, Phys. Rev. **93**, 99 (1954).  
 [2] R. Bonifacio and L. A. Lugiato, Phys. Rev. A **11**, 1507 (1975).  
 [3] A. V. Andreev, V. I. Emel'yanov, and Yu. A. Il'inskii, Sov. Phys. Usp. **23**, 493 (1980).  
 [4] M. F. H. Schuurmans, Q. H. F. Vreken, D. Polder, and H. M. Gibbs, in *Advances in Atomic and Molecular Physics*, edited by D. Bates and B. Bederson (Academic, New York, 1981), p. 167.  
 [5] Q. U. F. Vreken and U. M. Gibbs, in *Dissipative Systems in Quantum Optics*, edited by R. Bonifacio (Springer-Verlag, Berlin, 1982), p. 111.  
 [6] M. Gross and S. Haroche, Phys. Rep. **93**, 301 (1982).  
 [7] L. Allen and G. I. Peters, Phys. Lett. **31A**, 95 (1970); G. I. Peters and L. Allen, J. Phys. A **14**, 238 (1971).  
 [8] A. L. Schawlow and C. H. Townes, Phys. Rev. **112**, 1940 (1958).  
 [9] M. S. Feld, in *Frontiers in Laser Spectroscopy*, edited by R. Balian, S. Haroche, and S. Liberman (North-Holland, Amsterdam, 1977), Vol. 1, p. 203.  
 [10] R. G. Brewer and R. L. Shoemaker, Phys. Rev. Lett. **27**, 631 (1971).  
 [11] I. D. Abella, N. A. Kurnit, and S. R. Hartmann, Phys. Rev. **141**, 391 (1966).  
 [12] J. H. Eberly and N. E. Rehler, Phys. Lett. **29A**, 142 (1969); Phys. Rev. A **2**, 1607 (1970); N. E. Rehler and J. H. Eberly, *ibid.* **3**, 1735 (1971).  
 [13] R. J. Glauber and F. Haake, Phys. Rev. A **13**, 357 (1976).  
 [14] A review of SRS as an amplifier of quantum fluctuations is given by M. G. Raymer and I. A. Walmsley, Prog. Opt. **28**, 181 (1990).  
 [15] B. J. Herman, J. H. Eberly, and M. G. Raymer, Phys. Rev. A **39**, 3447 (1989); S. Kinoshita and T. Kushido, *ibid.* **42**, 2751 (1990).  
 [16] M. G. Raymer and J. L. Carlsten, Phys. Rev. Lett. **39**, 547 (1977).  
 [17] J. J. Maki, M. S. Malcuit, M. G. Raymer, R. W. Boyd, and P. D. Drummond, Phys. Rev. A **40**, 5135 (1989). See, in particular, Fig. 1.  
 [18] N. Skribanowitz, J. P. Herman, J. C. MacGillivray, and M. S. Feld, Phys. Rev. Lett. **30**, 309 (1973).  
 [19] H. M. Gibbs, Q. H. F. Vreken, and H. M. J. Hikspoors, Phys. Rev. Lett. **39**, 547 (1977).  
 [20] M. Gross, C. Fabre, P. Pillet, and S. Haroche, Phys. Rev. Lett. **36**, 1035 (1976).  
 [21] A. Flusberg, T. Mossberg, and S. R. Hartmann, Phys. Lett. **58A**, 373 (1976).  
 [22] A. T. Rosenberger and T. A. DeTemple, Phys. Rev. A **24**, 868 (1981); D. P. Scherrer and F. K. Kneubuhl, Infrared Phys. **34**, 227 (1993).  
 [23] A. Crubellier, S. Liberman, D. Mayou, and P. Pillet, Opt. Lett. **8**, 105 (1982).  
 [24] N. Beverini, F. Giammanco, E. Maccioni, F. Strumia, and G. Vissani, J. Opt. Soc. Am. B **6**, 2188 (1989).  
 [25] F. T. Arecchi and E. Courtens, Phys. Rev. A **2**, 1730 (1970).  
 [26] T. W. Karras, R. S. Anderson, B. G. Bricks, and C. E. Anderson, in *Cooperative Effects in Matter and Radiation*, edited by C. M. Bowden, D. W. Howgate, and H. R. Robl (Plenum, New York, 1977), p. 101.  
 [27] M. D. Rosen *et al.*, Phys. Rev. Lett. **54**, 106 (1985).  
 [28] D. L. Matthews *et al.*, Phys. Rev. Lett. **54**, 110 (1985).  
 [29] S. Suckewer, C. H. Skinner, H. Milchberg, C. Keane, and D. Voorhees, Phys. Rev. Lett. **55**, 1753 (1985).  
 [30] H. C. Kapteyn and R. W. Falcone, Phys. Rev. A **37**, 2033 (1988).  
 [31] M. Hogan, C. Pellegrini, J. Rosenzweig, G. Travish, A. Varfolomeev, S. Anderson, K. Bishofberger, P. Frigola, A. Murokh, N. Osmanov, S. Reiche, and A. Tremaine, Phys. Rev. Lett. **80**, 289 (1998).  
 [32] G. Banfi and R. Bonifacio, Phys. Rev. A **12**, 2068 (1975).  
 [33] R. Bonifacio, F. A. Hopf, P. Meystre, and M. O. Scully, Phys. Rev. A **12**, 2568 (1975).  
 [34] R. Bonifacio, P. Schwendimann, and F. Haake, Phys. Rev. A **4**, 302 (1971).  
 [35] R. Friedberg and S. R. Hartmann, Phys. Lett. **37A**, 285 (1971).  
 [36] M. F. H. Schuurmans, Opt. Commun. **34**, 185 (1980).  
 [37] E. Ressayre and A. Tallet, Phys. Rev. Lett. **30**, 1239 (1973).  
 [38] J. C. Garrison, H. Nathel, and R. Y. Chiao, J. Opt. Soc. Am. B **5**, 1528 (1988).  
 [39] M. S. Malcuit, J. J. Maki, D. J. Simkin, and R. W. Boyd, Phys. Rev. Lett. **59**, 1189 (1987).  
 [40] R. Bonifacio, J. D. Farina, and L. M. Narducci, Opt. Commun. **31**, 377 (1979).  
 [41] C. M. Bowden and C. C. Sung, Phys. Rev. A **18**, 1558 (1978); **20**, 2033 (1979).

- [42] W. L. Wiese, M. W. Smith, and B. M. Miles, *Atomic Transition Probabilities*, Natl. Bur. Stand. Ref. Data Ser., Natl. Bur. Stand. (U.S.) No. 22 (U.S. GPO, Washington, DC, in press), Vol. II.
- [43] L. P. Lellouch and L. R. Hunter, *Phys. Rev. A* **36**, 3490 (1987).
- [44] R. N. Diefenderfer, P. J. Dagdigan, and D. R. Yarkony, *J. Phys. B* **14**, 21 (1981).
- [45] T. Holstein, *Phys. Rev.* **72**, 1212 (1947); **83**, 1159 (1951).
- [46] A. Corney, in *Atomic and Laser Spectroscopy* (Oxford, New York, 1977), Chap. 10.
- [47] A. Kumarakrishnan, Ph.D. thesis, University of Idaho, 1992.
- [48] R. E. Honig and D. A. Kramer, *RCA Rev.* **30**, 285 (1969).
- [49] D. Polder, M. F. H. Schuurmans, Q. H. F. Vreken, *Phys. Rev. A* **19**, 1192 (1979).
- [50] X. L. Han (private communication); A. Kumarakrishnan, X. L. Han, and J. F. Kelly, *Bull. Am. Phys. Soc.* **35**, 1162 (1990).
- [51] R. Bonifacio, M. Gronchi, and L. A. Lugiato, *Coherence and Quantum Optics IV*, edited by L. Mandel and E. Wolf (Plenum, New York, 1978), p. 939; R. Bonifacio, M. Gronchi, L. A. Lugiato, and A. M. Ricca, in *Cooperative Effects in Matter and Radiation* (Ref. [26]), p. 193.
- [52] A. Kumarakrishnan, J. F. Kelly, and X. L. Han, *Bull. Am. Phys. Soc.* **38**, 1154 (1993).
- [53] J. F. Kelly, A. Kumarakrishnan, and X. L. Han, *Bull. Am. Phys. Soc.* **36**, 1953 (1991); A. Kumarakrishnan and X. L. Han (unpublished).
- [54] A. Kumarakrishnan and X. L. Han (unpublished).
- [55] D. J. Heinzen, J. E. Thomas, and M. S. Feld, *Phys. Rev. Lett.* **54**, 677 (1985).
- [56] A. Kumarakrishnan and X. L. Han, *Opt. Commun.* **109**, 348 (1994); J. F. Kelly, A. Kumarakrishnan, and X. L. Han, *Bull. Am. Phys. Soc.* **38**, 1154 (1993).
- [57] M. H. Anderson, J. R. Ensher, M. R. Matthews, C. E. Wieman, and E. A. Cornell, *Science* **269**, 198 (1995).
- [58] E. L. Raab, M. Prentiss, A. Cable, S. Chu, and D. E. Pritchard, *Phys. Rev. Lett.* **59**, 2631 (1987).